

## The fractal lung: Universal and species-related scaling patterns

T. R. Nelson<sup>a</sup>, B. J. West<sup>b</sup> and A. L. Goldberger<sup>c</sup>

<sup>a</sup>Department of Radiology, M-010, University of California, San Diego-La Jolla (California 92093, USA),

<sup>b</sup>Department of Physics, University of North Texas, Denton (Texas 76203, USA), and <sup>c</sup>Cardiovascular Division, Beth Israel Hospital, Harvard Medical School, 330 Brookline Ave, Boston (Massachusetts 02215, USA)

Received 15 June 1989; accepted 25 October 1989

**Summary.** The mammalian lung exhibits features of a fractal tree: heterogeneity, self-similarity and the absence of a characteristic scale. The finite nature of the lung ultimately limits the range over which self-similarity scaling characteristics are applicable. However, generalization based on the scaling features of fractals, provides unique insight into geometric organization of anatomic structures. Furthermore, the mathematical theory of renormalization groups provides a description of the harmonically-modulated inverse power-law scaling observed for bronchial tree dimensions observed in different species. Compared to several mammalian species (dog, rat, hamster), the human lung shows marked differences in the phase of the harmonic modulation for both length and diameter measurements. These inter-species scaling differences suggest that evolutionary factors modify certain universal features of morphogenesis.

**Key words.** Bronchial tree; evolution; fractal; lung airway; morphogenesis; renormalization group theory.

The mammalian lung airway is a progressively branching structure<sup>1-4</sup>. Although certain scaling properties have been well known for some time, Mandelbrot was the first to suggest that the airway structure of the lung is fractal<sup>4</sup>. Fractal concepts have subsequently been applied to a broad class of anatomic structures, including the vascular tree, neural networks, biliary and urinary ducts, brain and bowel folds, cardiac conduction fibers, as well as the bronchial airway<sup>5</sup>. Fractal objects lack a characteristic scale and demonstrate self-similarity; that is, their small-scale structure resembles their large-scale form. The finite nature of the lung ultimately limits the range over which self-similarity scaling characteristics are applicable. However, generalization based on the scaling features of fractals, provides unique insight into geometric organization of anatomic structures. The tracheo-bronchial tree is probably the best characterized of these anatomic fractals owing to the availability of detailed morphometric measurements made from a number of mammalian lung casts<sup>6</sup>.

The lung airway is most simply described as a dichotomous branching tree in which the parent tube bifurcates into two daughter tubes from the trachea to the terminal bronchioles<sup>1-3</sup>. Each branch point represents a new order or generation where the trachea is defined as order 0, the left and right mainstem branches as order 1, and so on<sup>1,2</sup>. Dichotomous branching means that the number of branch segments (N) in each successive order (z) increases as  $N = 2^z$ . The segment length and diameter in each order decreases, on average, with respect to the preceding order. In addition, the two daughter branches arising at a bifurcation usually differ in their length, diameter, and angle, with respect to the parent branch, leading to the highly heterogeneous, asymmetric architecture of the mammalian lung<sup>2,7-10</sup>.

Since the beginning of this century, considerable attention has been devoted to understanding scaling proper-

ties of the lung<sup>3</sup>. In particular, the mean dimensions of each bronchial generation and their relationship to the previous and successive generations have been studied in detail<sup>2,7-9</sup>. These scaling relationships have been described using conventional morphological techniques<sup>10</sup> as well as from the perspective of biophysical resources utilization<sup>11</sup>.

Classical models of airway scaling have been exponential, assuming a single characteristic scale factor<sup>1-3</sup>. That is, the mean diameter or length of each generation is a scaled down version of the previous one by a constant scaling fraction such that

$$S(z) = S(0) \alpha^z \quad (1)$$

where  $\alpha$  ( $\alpha < 1$ ) is the scaling factor,  $z$  is the branch order and  $S$  is the mean dimension of the  $z^{\text{th}}$  generation ( $S(0)$  is the tracheal dimension). The complexity of the bronchial tree structure however, requires more complete characterization than possible with a simple exponential model.

More recently, a model of the mammalian lung has been proposed based on the theory of renormalization groups that describes the architecture of fractal anatomies, such as the lung airway, based on a multiplicity of scales<sup>12</sup>. Rather than a single scale, the renormalization model incorporates a distribution of scaling functions represented by a probability function  $P(\alpha)$ <sup>12-16</sup>. When  $P(\alpha)$  has only a single scale then the data exhibit exponential scaling. This situation results for a regular branching tree where the size of the  $z^{\text{th}}$  branch is the same for all segments. On the other hand, for a heterogeneous branching tree, the size of each branch is dependent on preceding generations. A larger branch size derives from larger parent branches in earlier generations. Thus, if we define the different scales comprising the  $z^{\text{th}}$  generation by  $\alpha$ , then  $S(z)$  becomes  $S(z/\alpha)$  since the size is dependent on the

$z/\alpha^{\text{th}}$  generation. For the  $z^{\text{th}}$  generation, we have a range of scales present with  $P(\alpha)$  defining the distribution of scales and  $S(z)$  given by

$$S(z) = \int_0^{\infty} S(z/\alpha) P(\alpha) d\alpha \quad (2)$$

where  $P(\alpha)$  determines the functional form of the size distribution. Thus, for a given  $P(\alpha)$ , the mean airway dimension ( $S(z)$ )(diameter, length, volume) should decline, not as an exponential, but as an inverse power-law modulated by a harmonic (periodic) function in which the size of branch segment ( $S(z)$ ) is now given by <sup>12</sup>:

$$S(z) = z^{\mu} A(z) \quad (3)$$

where:

$$A(z) = \sum_{n=-\infty}^{\infty} A_n \exp \left[ \frac{\{2\pi i n \ln(z)\}}{\ln(\lambda)} \right] \quad (4)$$

where:  $\ln(z)$  is the period of modulation with fundamental period  $\ln(\lambda)$ ,  $\lambda$  defines the overall range of scales over which  $P(\alpha)$  applies,  $\mu$  is the power law index which is related to the fractal dimension, and  $A_n$  are the relative weights of the harmonic terms used to fit the data.

The current work extends previous work by West et al.<sup>12</sup> and presents new observations regarding scaling similarities among four mammalian species with respect to airway length, diameter and branching order. Furthermore, we describe a novel method for quantitating inter-species variations in lung morphometry based on a comparison of the harmonic terms in Eq. 4. Differences in the airway geometry between mammalian species are readily measured via the harmonic scaling ( $A(z)$ ) terms of the renormalization group model and are expressed as a phase shift. In turn, these phase shifts highlight previously unrecognized differences between the human lung and certain other mammalian species.

Our analysis utilizes bronchial airway data compiled by Raabe and associates derived from silicone lung casts of several individuals for each of four species: human, rat, dog, and hamster<sup>6,10</sup>. We present results for a single individual from each species although data from other individuals exhibited similar scaling characteristics. The technique for producing the airway casts was as follows; briefly silicone rubber was injected through the trachea into the airway of a lung (in situ). The silicone was allowed to set, the lung was removed from the thorax, and the tissue digested yielding a replica cast of the airway from trachea to alveoli. The length and diameter were measured for branch segments from the trachea to the terminal bronchioles and cataloged using a numbering system that unambiguously identified the location of all tracheo-bronchial segments. Stereoradiographic evaluation of the casts confirmed an end-inspiratory state of

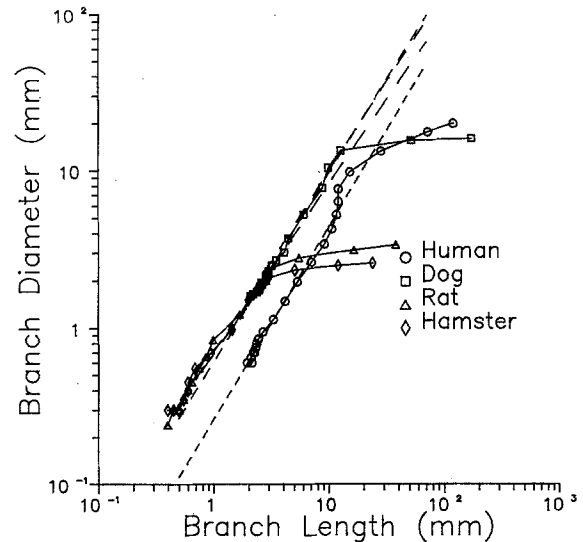


Figure 1. Plot of the mean branch diameter versus the mean branch length for the four species. Each point represents one bronchial order ( $z$ ) where the trachea ( $z = 0$ ) is the rightmost point. After the initial few orders all species demonstrate similar inverse power-law scaling relationships between mean branch diameter and length (see also table).

inflation and indicated a size variation of less than 10% when compared to in vivo values<sup>10</sup>.

Certain apparently universal features of lung scaling that transcend speciation can be readily appreciated from by reanalyzing the original data of Raabe et al. Figure 1 shows a plot of the mean branch length versus mean branch diameter with data points given for each branch order for the four species. After the first few orders, the data points for each lung cast lie on a straight line of the log-log graph, indicating a power-law relationship. Furthermore, the slopes of the regression lines (table) are similar for all four species<sup>17,18</sup>. These data indicate that the relationship between mean airway diameter and mean length is relatively constant over many orders for different species.

Figure 2 depicts the mean airway length versus bronchial order for the four species. As previously reported<sup>12</sup> the data points for all four species are well fit by a harmonically modulated, inverse power-law function. There is, however, a striking difference in the phase of the harmonic modulation between the human data set and those of the other species. Quantitative assessment of the relative phase between the human and animal bronchial length data (table and fig. 3) indicates a mean phase difference of approximately  $172^\circ$  (range:  $159^\circ$ – $183^\circ$ ). Similar plots for diameter data from the four species are presented in figures 4 and 5 and in the table. Although the diameter data from all four species are well fit by a harmonically modulated inverse power-law model (table and fig. 5), important phase differences are again apparent between the human lung and those of other species mean  $75^\circ$  (range:  $68^\circ$ – $84^\circ$ ).

These findings are of interest for several reasons. Analysis of mammalian lung airway dimensions reveals a rela-

Airway scaling relationships

	Human	Dog	Rat	Hamster
Length/diameter				
Intercept	$0.26 \pm 0.02$	$0.60 \pm 0.03$	$0.70 \pm 0.06$	$0.69 \pm 0.07$
Slope	$1.23 \pm 0.04$	$1.20 \pm 0.04$	$1.15 \pm 0.14$	$1.08 \pm 0.18$
(orders 4–16)				
Length				
Inverse power intercept (mm)	$138.5 \pm 0.8$	$128.3 \pm 0.8$	$37.4 \pm 0.8$	$22.8 \pm 0.8$
Slope	$-1.38 \pm 0.01$	$-1.43 \pm 0.01$	$-1.59 \pm 0.02$	$-1.37 \pm 0.02$
Harmonic phase shift (°)	25	-158	-134	-149
(orders 4–16)				
Diameter				
Inverse power intercept (mm)	$40.7 \pm 0.7$	$23.8 \pm 0.5$	$6.5 \pm 0.6$	$4.5 \pm 0.5$
Slope	$-1.26 \pm 0.01$	$-0.86 \pm 0.01$	$-1.05 \pm 0.04$	$-0.90 \pm 0.05$
Harmonic phase shift (°)	-25	-109	-93	-99
(orders 4–16)				

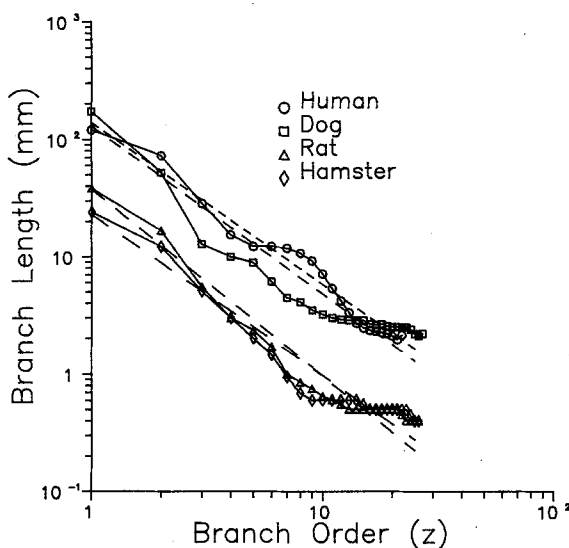


Figure 2. Plot of mean branch length versus branch order for four species. All four data sets show a harmonic modulation around the inverse power-law regression (broken line) with a fit of the form: Length = Intercept \* Order<sup>Slope</sup>. The value of slopes and intercepts are given in the table. Note: a pure inverse power-law behavior will be represented as a straight-line plot on a log-log graph. The harmonic modulation incorporated in the renormalization model results in an oscillation around the inverse power-law fit. There is a marked difference in phase between human airway data and that of the other three species (table).

tively constant relationship between mean airway length and diameter for different species (fig. 1). The observation of scaling universalities in a complex structure such as the lung, is not surprising given the constraints imposed by optimizing resource utilization requirements<sup>11</sup>. Furthermore, the harmonically-modulated inverse power-law behavior of the bronchial dimension versus branch order supports the usefulness of the renormalization group model in modeling features of the bronchial airway scaling<sup>12,14</sup>. The renormalization model, because it incorporates a multiplicity of scales, also has been shown to be more robust and error tolerant than exponential models that incorporate only a single scale<sup>15</sup> suggesting potential developmental advantages of 'fractal morphogenesis'.

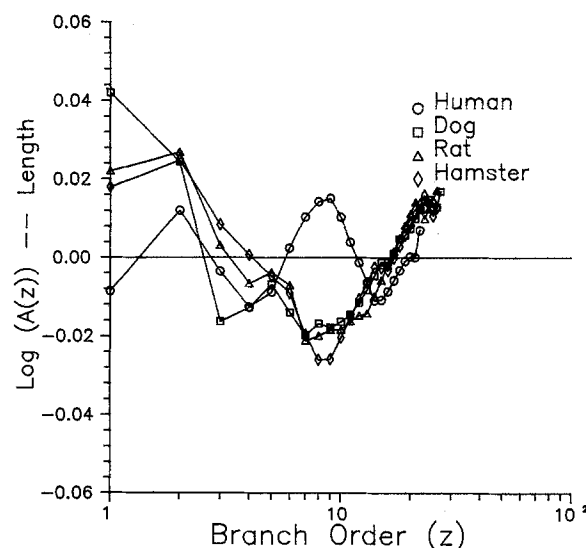


Figure 3. Detailed plot of harmonic variation in mean branch length [A(z)] from figure 2 with the inverse power-law behavior [z<sup>s</sup>] removed. The difference between the inverse power-law fit and the original data is ln[A(z)]. Note the approximately 180° discrepancy in mean phase between the data points from the human lung and the other three species (table).

At the same time, other features, notably variations in the harmonic scaling in bronchial dimension with branch order, reveal important species-related differences. Most apparent are the disparities in the phase of the harmonic modulation between the human and other mammalian bronchial airways. While structurally the human airway undergoes relatively little change in branch length for orders 5 through 10, the other species (dog, rat, and hamster) undergo a large change in length for the same branch orders. In contrast, these animal species demonstrate relatively little change in branch length or diameter from orders 13 onward while the human lung demonstrates a large change in length over the same orders. Consideration of the volume occupied by the lung by itself does not explain these differences. Bronchial scaling

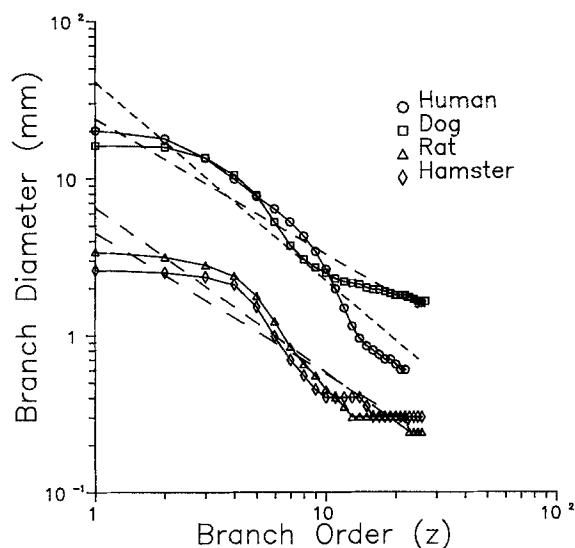


Figure 4. Plot of mean branch diameter versus branch order for four species. All four data sets show a harmonic modulation around the inverse power-law regression (broken line) with a fit of the form: Diameter = Intercept \* Order<sup>Slope</sup>. The value of slope and intercept are given in the table. (Compare with fig. 2)

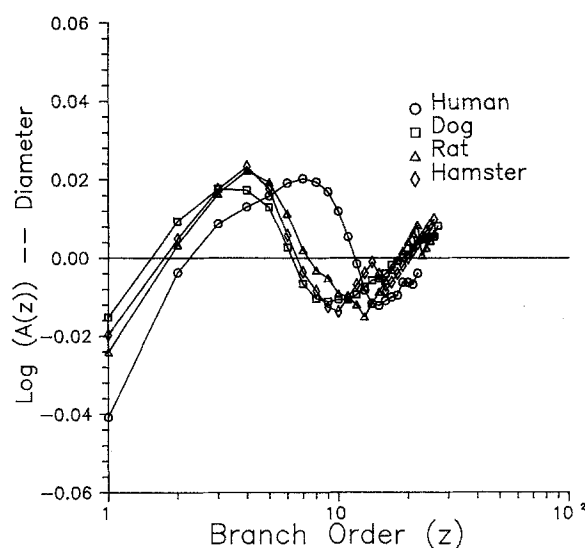


Figure 5. Detailed plot of harmonic variation in mean branch diameter  $[A(z)]$  from figure 4 with the inverse power-law behavior  $[z^{\text{slope}}]$  removed. The difference between the inverse power-law fit and the original data is  $\ln[A(z)]$ . A mean relative phase difference of  $75^\circ$  is present between the human and other species (table). (Compare with fig. 3)

in the dog, rat, and hamster are remarkably similar (figs 1–5) despite rather large differences in their lung volumes.

The scaling differences between the human and these other mammalian species may be related to postural orientation; quadruped versus biped. However, the selection advantages conferred by a particular scaling pattern remains to be elucidated. Prospective analysis of scaling patterns from lung casts of other mammalian species will be useful in testing this postural hypothesis. Quantitative characterization of other fractal anatomies (e.g. vascular trees) using the renormalization model also may be of interest from an evolutionary as well as physiological perspective.

**Acknowledgments.** This work supported in part by grants to A. L. Goldberger from the National Heart, Lung and Blood Institute (RO1 HL42172) and the G. Harold and Leila Y. Mathers Charitable Foundation.

- 1 Weibel, E. R., and Gomez, D. M., *Science* 127 (1962) 577.
- 2 Weibel, E., *Morphometry of the Human Lung*. Academic Press, New York 1963.
- 3 Rohrer, F., *Pflügers Arch.* 162 (1915) 225.
- 4 Mandelbrot, B., *The Fractal Geometry of Nature*. W. H. Freeman and Company, New York 1983.

- 5 Goldberger, A. L., and West, B. J., *Yale J. biol. Med.* 60 (1988) 421.
- 6 Raabe, O., Yeh, H., Schum, G., and Phalen, R., *Tracheobronchial Geometry: Human, Dog, Rat, Hamster (LF-53)*. Government Printing Office, Washington, DC 1976.
- 7 Horsfield, K., and Cumming, G., *J. appl. Physiol.* 24 (1968) 373.
- 8 Horsfield, K., Dart, G., Olson, D., Filley, G., and Cumming, G., *J. appl. Physiol.* 31 (1971) 207.
- 9 Parker, H., Horsfield, K., and Cumming, G., *J. appl. Physiol.* 31 (1971) 386.
- 10 Phalen, R., Yeh, H., Schum, G., and Raabe, O., *Anat. Rec.* 190 (1978) 167.
- 11 MacDonald, N., *Trees and Networks in Biological Models*. Wiley, New York 1983.
- 12 West, B. J., Bhargava, V., and Goldberger, A. L., *J. appl. Physiol.* 60 (1986) 1089.
- 13 Shlesinger, M. F., and Hughes, B. D., *Physica* 109A (1981) 597.
- 14 West, B. J., and Goldberger, A. L., *Am. Scient.* 75 (1987) 354.
- 15 West, B. J., *Fractals Intermittency and Morphogenesis*, in: *Chaos in Biological Systems*. Eds H. Degen, A. V. Holden and L. F. Olsen. Plenum, New York 1987.
- 16 Montroll, E. W., and Shlesinger, M. F., *J. stat. Phys.* 32 (1983) 209–230.
- 17 Bevington, P. R., *Data Reduction and Error Analysis for the Physical Sciences*. McGraw-Hill, New York 1969.
- 18 Press, W. H., Flannery, B. P., Teukolsky, S. A., and Vetterling, W. T., *Numerical Recipes*. Cambridge University Press, New York 1986.